

REMOTE SENSING OF SEASONAL AND ANNUAL VARIATION OF EQUATORIAL NEW PRODUCTION: A MODEL FOR GLOBAL ESTIMATES

R. Dugdale,* F. Wilkerson,* D. Halpern,** F. Chavez,*** and R. Barber†

*Department of Biological Sciences, University of Southern California, Los Angeles, CA 90089, USA. **Jet Propulsion Laboratory of California Institute of Technology, Pasadena, CA 91109, USA. ***Monterey Bay Aquarium Research Institute, Pacific Grove, CA 93950, USA. †Duke University Marine Laboratory, Pivers Island, Beaufort, NC 28516, USA.

ABSTRACT

Sea-surface temperatures (SSTs) are strongly correlated with surface nitrate concentrations in coastal upwelling regions. Upwelling also occurs in the equatorial Pacific; correlations between temperature and nitrate concentration are strong. The University of Miami weekly averaged Advanced Very High Resolution Radiometer (AVHRR) SST data for October 1986 through June 1989 have been used to compute surface nitrate concentrations from 90° - 180°W and from 15°S - 15°N. The surface areas with nitrate above detection limits are combined with existing nitrate uptake data to give weekly estimates of equatorial new production.

INTRODUCTION

The deep water of the ocean is a huge reservoir of the oxidised forms of nitrogen and phosphorus, i.e., nitrate and phosphate, which occur in the ratios required for phytoplankton growth in the euphotic zone, and inorganic carbon, which occurs in great excess of phytoplankton requirements. When deep water is carried into the euphotic zone, phytoplankton growth consumes the newly available nitrate, phosphate, and inorganic carbon in a process called new production /1/. The unused inorganic carbon becomes available for transfer to the atmosphere if the partial pressure of carbon dioxide in the ocean near the sea surface is greater than in the atmosphere near the sea surface.

Chavez and Barber /2/ reported that the proportion of world ocean new production in 180° - 90°W, 5°N - 5°S eastern equatorial Pacific was 10% to 56%. One of the dominant reasons for the large uncertainty was that their limited data were not representative of the natural spatial and temporal variations. The El Niño and La Niña episodes produce large interannual variations. Along the Pacific equator, the strength of upwelling has large seasonal fluctuations /3/ and spatial variations /4/.

The enormous area of the equatorial Pacific makes it certain that shipboard measurements alone can not provide adequate areal estimates of new production with a minimal amount of aliasing. Only satellites provide adequate spatial and temporal coverage. As surrogate for satellite-derived measurements of new production, the remotely sensed sea-surface temperatures available from AVHRR can be used, through the model presented in this communication.

METHODOLOGY

We use remotely sensed sea-surface temperatures (from polar orbiting satellites) to estimate sea-surface nitrate. Surface nitrate is a good indicator of potential new production, the area of potential new production being defined as the area within which the surface nitrate concentration is detectable by standard colorimetric analyses (i.e., greater than $0.1 \mu\text{M}$ /5/).

Weekly averaged sea-surface temperatures from the University of Miami/Rosenstiel School of Marine and Atmospheric Sciences MCSST were obtained from the NASA Ocean Data System /6/. The data extracted for this study were in a box bounded by $180^\circ - 90^\circ\text{W}$ and $15^\circ\text{N} - 15^\circ\text{S}$. Weekly data from this area with a spatial resolution of 18 km were processed for images from October 1986 to July 1989. These temperatures were converted to sea-surface nitrate concentrations using regressions of nitrate and temperature from shipboard measurements from 1986 for the same area of the equatorial Pacific (i.e. from $180^\circ - 90^\circ\text{W}$), $15^\circ\text{N} - 15^\circ\text{S}$. Different regressions were obtained for different sectors of the area (Table 1), so the appropriate regression equation was applied to each pixel with a linear interpolation between the values of intercept and slope for each line in the image.

TABLE 1 Linear Regression Data for Shipboard Acquired Nitrate versus Temperature for the Equatorial Pacific during 1986

Sector	Intercept	Slope	r^2
$1^\circ\text{N} - 1^\circ\text{S}$	53.86	-1.86	.97
$1^\circ\text{N} - 5^\circ\text{N}$	59.11	-2.11	.97
$1^\circ\text{S} - 5^\circ\text{S}$	59.11	-2.11	.97
$5^\circ\text{N} - 15^\circ\text{N}$	60.45	-2.03	.92
$5^\circ\text{S} - 15^\circ\text{S}$	50.43	-1.84	.87

$$[\text{NO}_3] = \text{intercept} - \text{slope} * \text{temperature}$$

The nitrate concentrations were written back to standard 9 track tape and deposited at the NASA Ocean Data System. The data were then ingested into the SEAPAK package /7,8/ in a PC where all of the procedures of that system are available for further data analysis (i.e. averaging, imaging etc). Color images of the nitrate field for each week were produced, printed out to hard copy and saved as image files. A video has been made of each of the weekly images providing a time-lapse presentation of the changes that occurred during the period of study.

Originally we hoped to use a physiological model developed for coastal

upwelling systems /9,10/ to determine realized new production using the temperature field to estimate the nitrate field and time series upwelling. Our recent research has shown that the phytoplankton productivity in the equatorial Pacific may not respond in the same way to upwelling as in coastal upwelling ecosystems /11,12,13/ and can be described as an HNLC (high nutrient, low chlorophyll) region /14/, consequently this model cannot be applied. Instead, estimates of total areal integrated new production for each week of the data have been made by by summing the pixels in which nitrate concentrations are greater than 1.5 μM , computing the area of sea surface represented by these pixels and multiplying by the mean new production rate for the area (47.5 $\text{mg C m}^{-2} \text{d}^{-1}$) observed in field studies at 150°W on the WECOMA 88 cruise (Table 4; /11/). The 1.5 μM concentration boundary was arbitrarily chosen to match the lowest range used in the color images, since the bottom concentration bracket used to prepare the images was 0-1.5 μM .

RESULTS

Validation of the Model

The computed nitrate distributions obtained from AVHRR-sensed temperatures were compared with a different shipboard nitrate data set for the area. Computed nitrate data was extracted for each location and time (i.e. within the corresponding week) where shipboard data was available. The extracted ship-acquired data were compared with the computed data (mean of 3 pixels, one to the west and one to the east of the central pixel of the location) with linear regression. The data were treated in two ways, for all areas between 170° - 109°W, 15°N - 5°S, and for the equatorial swath, 2°N - 2°S, alone (Table 2).

TABLE 2 Linear Regressions of Shipboard Acquired Nitrate Data versus Satellite Acquired Nitrate Data from 1988

Data Used	Intercept	Slope	r^2	n
Entire available data 170° - 109°W, 15°N - 5°S	4.92	0.66	0.48	129
Equatorial swath data 170° - 109°W, 2°N - 2°S	3.79	0.90	0.43	48

Both approaches give similar r^2 (0.48 and 0.43) that are respectable since the shipboard data used were for 1988 (a La Niña condition following an El Niño year) and their spatial extent was only to 5°S while the regressions used to estimate nitrate from remotely sensed SST (Table 1) were based on 1986 data and extended to 15°S. The regression equations used for the northernmost sector apparently overestimate the surface nitrate concentration and adjustments to the equations must eventually be made for that region. The slope of 0.9 for the equatorial swath is reasonably close to the ideal slope of 1.0. The intercept, 3.79 μM nitrate, indicates a tendency for the satellite derived nitrate to overestimate the measured values. However, the r^2 of 0.43 indicates a high degree of scatter in the data which is not unexpected given the temporal variability in the equatorial upwelling system and the instantaneous nature of the shipboard data and the weekly averaging of the satellite data. Also the 18 km resolution within the MCSST data may add to the variability. The full data set combined for the region resulted in a poorer fit of the slope, 0.66, to the ideal slope and a slightly higher intercept 4.92 μM nitrate. The shipboard data used for 1988 were for a

La Niña or exceptionally cold period and it may be that the regression equations may not be the same as for the more normal year, 1986. An underestimate of temperature would bias our estimate of nitrate concentration. The underestimate of temperature that would cause an overestimate of $3.49 \mu\text{M}$ can be calculated from the slope of the regression equation for $1^\circ\text{N} - 1^\circ\text{S}$ (Table 1) since the slope b is described by:

$$b = \Delta\text{NO}_3/\Delta T$$

and rearranged

$$\Delta T = \Delta\text{NO}_3/b = 3.49/-2.11 = -1.65^\circ\text{C}.$$

Color Images of Sea-surface Nitrate

Examples of the color images of the sea-surface nitrate concentrations are shown in Fig. 1. This shows four images that are from 2 different seasons (April and September) in two different years (1987 and 1988). All the images show enhanced nitrate at the equator. Fig. 1a shows low nitrate concentrations throughout most of the equatorial swath with some enhancement in surface nitrate at the eastern edge of the box. By September, the nitrate levels in Fig. 1b are much higher than in April 1987, illustrating the normal seasonal cycle in equatorial upwelling. The same seasonal trend is seen in the 1988 images (Figs 1c and d). Comparing the April and September images (ie. Figs 1a and 1c; Figs 1b and 1d) shows two extremes are represented in the data, the warm 1987 El Niño, and the 1988 colder than average, La Niña. Viewing the nitrate field on this areal and temporal scale reveals features not seen during cruises. The wavelike structure apparent in Figs 1b, c and d, are related to the 20-30 day waves first described by Legeckis /15/.

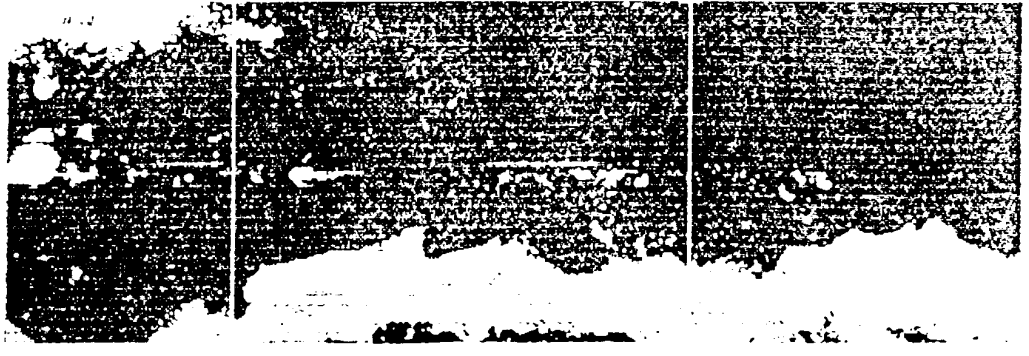
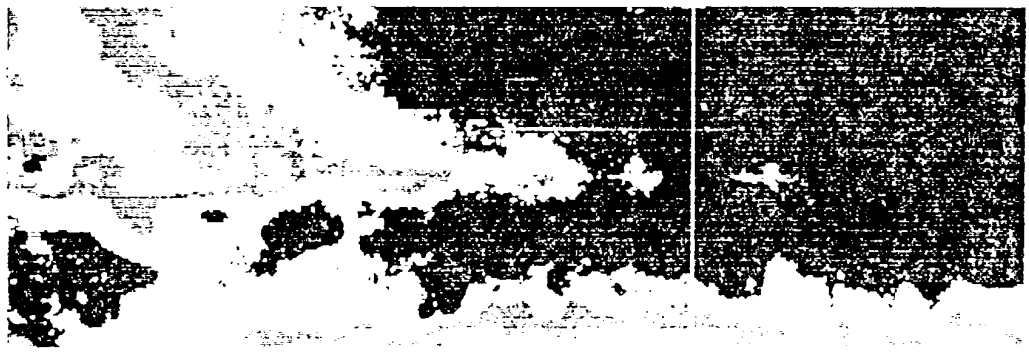
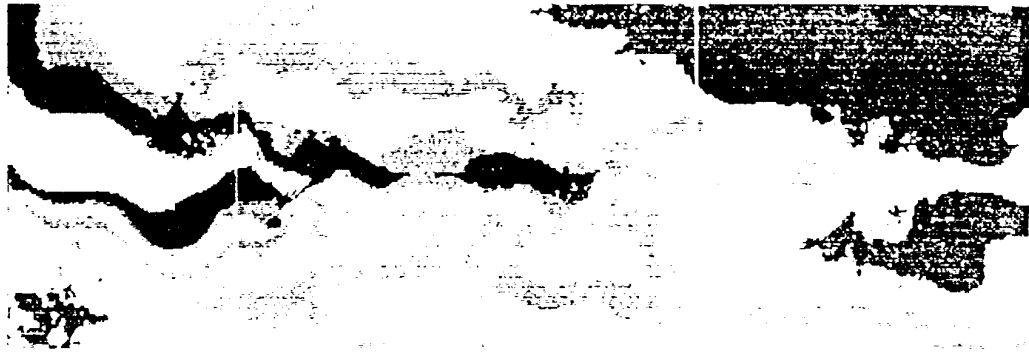
Nitrate Sections

Following computation of nitrate concentration for each week, the nitrate values at each pixel can be extracted and sections plotted (Fig. 2). This was carried out for 150°W and 110°W for the four periods shown in Fig. 1. For each degree longitude there are 5 pixels, the data from the central pixel is plotted going from $6^\circ\text{N} - 6^\circ\text{S}$. The same trend can be seen as displayed in the color images but this type of quantitative data can be compared with shipboard transects or be used for planning transects in future cruises. These remotely sensed surface transects emphasize certain features of the equatorial system, e.g. the highest concentrations occur at 110°W (note change in Y axis scale for nitrate concentration), the asymmetrical distribution of high nitrate (higher and farther to the south), and the tendency of the La Niña to be evidenced first in the easternmost end of the equatorial swath.

Time series of Surface Nitrate at the Equator

In a similar way the nitrate values at the equator (0°) for the central pixel for 150°W and 110°W can be extracted from each of the sequential weekly images. The resultant time series from January 1987 to July 1989 is shown in Fig. 3. Equatorial nitrate concentrations at 110°W are greater than at 150°W . The 1987 El Niño is evidenced by low nitrate values- particularly at 150°W . Towards the end of 1987 as the El Niño ends and the cooling La Niña begins surface nitrate at the equator rises rapidly reaching peak values (almost $20 \mu\text{M}$ at 110°W and $12 \mu\text{M}$ at 150°W by mid 1988. The values then decline and by 1989 the values at both lines of longitude are midway between the low El Niño and high La Niña concentrations.

Fig. 1. Nitrate distributions deduced from AVHRR SST data and empirical nitrate-temperature correlations. The box extends from 180° - 90°W, 15°N - 15°S. Yellow lines are drawn at 150°W and 110°W. Low nitrate is colored blue and high concentrations are red. a) week 16 (April), 1987; b) week 36 (September), 1987; c) week 16 (April), 1988 and d) week 34 (September), 1988.



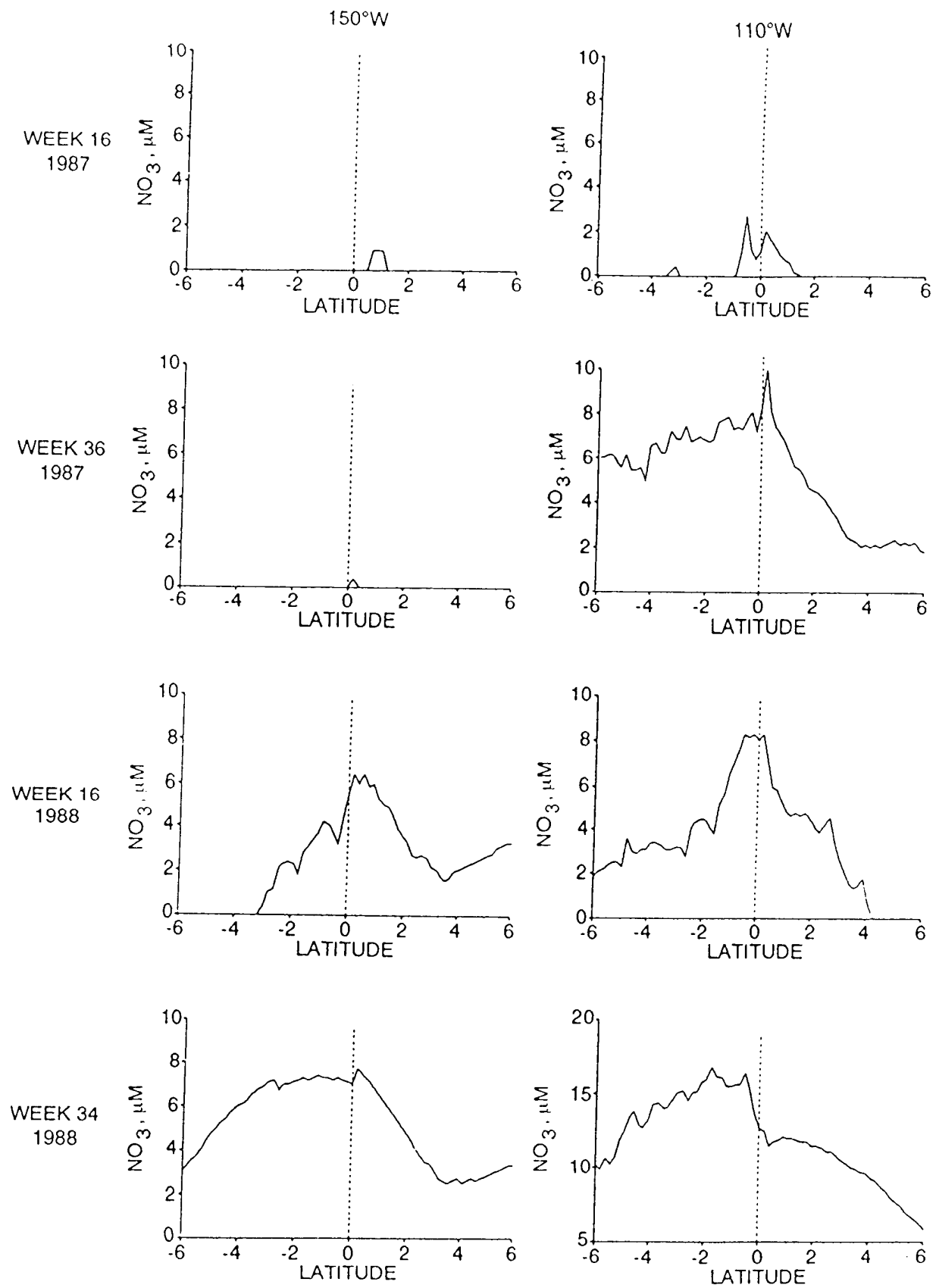


Fig. 2. Transects of surface nitrate concentrations (in μM) from 6°N - 6°S at 150°W and 110°W for the weeks shown in Figure 1.

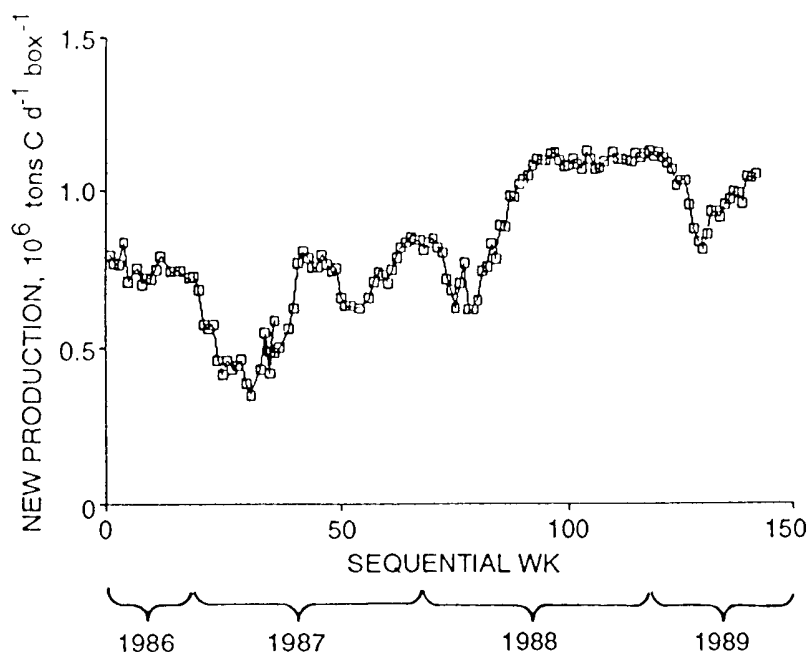


Fig. 3. Time series of surface nitrate at 0°, 150°W and 110°W from January 1987 to July 1989.

New Production Estimates

Estimates of areal new production can be made for each weekly image for the boxed area from 15°N - 15°S (180° - 90°W), 15°N - 15°S, using the number of pixels with measurable nitrate (i.e. greater than 1.5 μ M and a value for mean new production. Using a boundary of 1.5 μ M concentration boundary rather than a lower one fixed by analytical detection limits compensates at least partly for the apparent overestimate of NO_3 concentrations, 3.49 μ M suggested by the

TABLE 3 New Production Estimated from Weekly Averaged AVHRR-derived Measurements of SST, for the Area 180°-90°W, 15°N-15°S

Year, Julian Days	10^6 tons C d^{-1} mean \pm sd	n	10^{14} g C y^{-1}
1986, 274-365	0.75 \pm 0.04	12	2.73
1987, 1-364	0.63 \pm 0.13	47	2.29
1988, 1-363	0.95 \pm 0.17	51	3.46
1989, 1-179	1.00 \pm 0.91	26	3.65
Chavez and Barber, 1987*			2.70

* Use C fixation value * f , using $f = 0.14$ correction from Dugdale et al. /11/

comparison of 1988 shipboard analyses and the values computed from satellite temperatures using regression equations based on shipboard data. These estimates (Table 3) are crude and further modifications of the technique are in progress, but do provide insight into the variability of new production over the 3 year period (Fig. 4). There is a drop in productivity just after the start of each year (mid to late January). This figure also illustrates the low values of the 1987 El Niño compared to the higher values in 1988. The mean values for each year also show this well (Table 3). In this table we have compared our estimates with Chavez and Barber /2/. We have recalculated their data using percent new production, $f = 0.14$ (from data rather than apply their original model derived value of $f = 0.44$ (/16/)). When this recalculation is made our estimates and mean value for the 4 years, $3.03 \times 10^{14} \text{ g C y}^{-1}$, compare well with the Chavez and Barber (1987) estimate of $2.7 \times 10^{14} \text{ g C y}^{-1}$. Our estimates include some bias on the high side due to our use of a wider swath. However, the effect is limited largely to the area north of 5°N where our data suggest measurable surface nitrate concentrations occur while shipboard observations suggest none to be present.

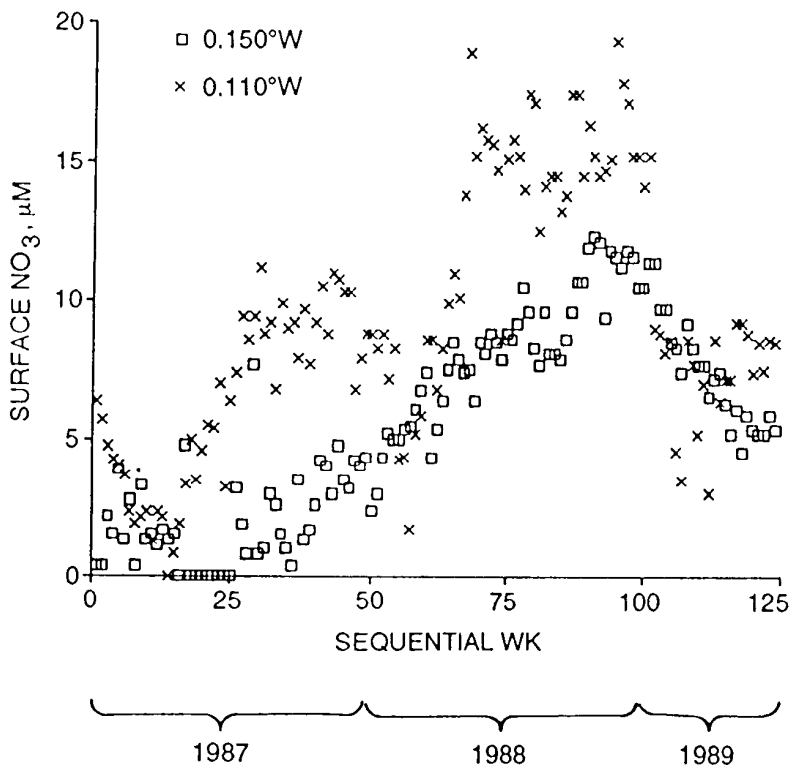


Fig. 4. Areal estimates of new production for the box $180^\circ - 90^\circ\text{W}$, $15^\circ\text{N} - 15^\circ\text{S}$ from June 1986 to July 1989 obtained from pixels with nitrate greater than $1.5 \mu\text{M}$ derived from SST data.

DISCUSSION

From these preliminary efforts we have found considerable encouragement for future research on the estimation of surface nutrient concentrations and new production from satellite derived sea-surface temperatures. Specifically, we have demonstrated that weekly averaged estimates of surface nitrate can be obtained from sea-surface temperatures from the Miami MCSST data set by conversion using nitrate-temperature regression coefficients. The remotely-sensed estimates of nitrate agree reasonably well with shipboard measurements. From each weekly

averaged image of sea-surface temperature, nitrate values that are produced can be extracted and used in a number of ways. We have illustrated how meridional transects at 150°W and 110°W can be constructed and how an annual time series of nitrate at a single location can be extracted. Such uses allow the data to be viewed and compared seasonally and annually at different spatial regimes. Large scale anomalies such as El Niños can be viewed with this capability (e.g. /16/) that would normally require many days at sea for such coverage in both time and space. The nitrate data can be used by itself to examine variability in the eastern equatorial Pacific. It can also be used to make estimates of new and total production. Changes in new production estimated from the total surface area with nitrate concentrations above a threshold detectability concentration of 1.5 μM agree well with the seasonal and interannual patterns of equatorial upwelling and surface nitrate concentrations. Our satellite derived estimates of equator-wide annual new production agree well with previous estimates based on ^{14}C primary productivity estimates, corrected by recent direct measurements of the ratio of new to total production.

We plan to refine the equatorial Pacific nitrate data with regressions obtained for the different seasons and years represented in both the MCSST data and the shipboard acquired nutrient data set and with regression parameters from additional high quality nutrient data sets from the eastern equatorial Pacific. Additional MCSST data sets now are available for 1981 through 1991 and these data will be processed to obtain longer time series of nitrate fields and new production estimates for the equatorial Pacific.

REFERENCES

1. R.C. Dugdale, R.C. and J.J. Goering, Uptake of new and regenerated forms of nitrogen in primary productivity, *Limnol. Oceanogr.* 12, 196, (1967).
2. F.P. Chavez and R.T. Barber, An estimate of new production in the equatorial Pacific, *Deep-Sea Res.* 34, 1229, (1987).
3. D. Halpern and G.C. Feldman, Annual and interannual variations of phytoplankton pigment concentration and upwelling along the Pacific equator, In press, (1992).
4. D. Halpern, R.A. Knox, D.S. Luther and S.G.H. Philander, Estimates of equatorial upwelling between 140° and 110°W during 1984, *J. Geophys. Res.* 94, 8018, (1989).
5. J.D.H. Strickland and T. Parsons, *A Practical Handbook of Seawater Analysis*, Bull. 167, Fish. Res. Bd. Canada, 1972.
6. D. Halpern, The NASA Ocean Data System at the Jet Propulsion Laboratory, *Advances in Space Res.* 11, (1991).
7. C. McClain, G. Fu, M. Darzi and J. Firestone, *PC-SEAPAK Users Guide*, NASA/GSFC Laboratory for Oceans, 1989.
8. J.K. Firestone, G. Fu, M. Darzi and C.R. McClain, NASA's Seapak software for oceanographic data analysis: an update, in: *Sixth Int. Conf. Interactive Inf. Processing Systems*, AMS. 1990, p. 260.

9. R.C. Dugdale, A. Morel, A. Bricaud and F.P. Wilkerson, Modeling new production in upwelling centers: II A case-study of modeling new production from remotely sensed temperature and color, *J. Geophys. Res.* 94, 18119, (1989).
10. R.C. Dugdale, F.P. Wilkerson and A. Morel, Modeling new production in upwelling centers: I Applications of a shift-up model to 3 upwelling areas, *Limnol. Oceanogr.*, 35, 822, (1990).
11. R.C. Dugdale, F.P. Wilkerson, R.T. Barber and F.P. Chavez, Estimating new production in the equatorial Pacific Ocean at 150°W, *J. Geophys. Res.* 97, 681, (1992).
12. R.C. Dugdale and F.P. Wilkerson, Nutrient limitation of new production, in: *Primary Productivity and Biogeochemical Cycles in the Sea*, eds. P.G. Falkowski and A.D. Woodhead, Plenum Press, New York, 1992, p. 107.
13. S.R. Yang, *Factors Controlling New Production in the Equatorial Pacific*, PhD Thesis, University of Southern California, 1992.
14. H.J. Minas and M. Minas, Net community production in "high nutrient low chlorophyll" waters off the tropical and Antarctic Oceans: grazing vs. iron hypothesis, *Oceanologica Acta*, 15, 145, (1992).
15. R. Legeckis, Long waves in the eastern equatorial Pacific ocean: a view from a geostationary satellite, *Science*, 197, 1181, (1977).
16. R.W. Eppley and B.J. Peterson, Particulate organic matter flux and planktonic new production in the deep ocean. *Nature* 282, 677, (1979).
17. R.T. Barber and F.P. Chavez, Ocean variability in relation to living resources during the 1982-83 El Niño. *Nature* 319, 279, (1986).